Journal of Engineering Science and Technology
6th EURECA 2016 Special Issue May (2017) 29 - 42

SYNTHESIS OF ZINC OXIDE NANOPARTICLES USING LIQUID-PHASE LASER ABLATION AND ITS ANTIBACTERIAL ACTIVITY

JANICE LOW J.-N.[1], WONG W. Y[1,*], RASHMI W.[1], KADHUM A. A. H.[2,3], MOHAMAD A. B.[2, 3]

[1]Energy Research Group, School of Engineering, Taylor's University, Taylor's Lakeside Campus, No. 1 Jalan Taylor's, 47500, Subang Jaya, Selangor, Malaysia
[2]Fuel Cell Institute, Universiti Kebangsaan Malaysia, 43600 UKM Bangi, Selangor, Malaysia
[3]Department of Chemical & Process Engineering, Faculty of Engineering and Built Environment, UniversitiKebangsaan Malaysia, 43600 UKM Bangi, Selangor, Malaysia
*Corresponding Author:waiyin.wong@ukm.edu.my

Abstract

The potential of zinc nanoparticles in various fields such as drug delivery, cancer treatment and food packaging has drawn great interest to the researchers in order to search for alternative production method with simpler set up. Antibacterial activities of zinc oxide nanoparticles were shown promising owing to its antibacterial properties over a wide range of bacteria strains and non-toxicity. In recent years, liquid-phase laser ablation was introduced as a modified method from conventional laser ablation with the advantage of providing a rapid quenching effect on the ablated metal surface, concurrently enable the ease of collection of metal nanoparticles ablated from the metal surface in the liquid medium. In most of the literature studies, the type of laser used for liquid-phase laser ablation of metal is Nd:YAG laser. For the first attempt, ytterbium fibre laser was used in this study for the liquid-phase laser ablation on zinc target to produce zinc oxide nanoparticles and its antibacterial activities will be investigated. In this study, the ablation parameters of laser power, frequency and ablation period were optimised to achieve zinc oxide with nano size. The nanoparticles were investigated on their particle size distribution using Zeta Sizer, morphology using TEM analysis, concentration using AAS analysis and antibacterial properties using agar disc diffusion with the presence of *E. coli*. The results show ZnO nanoparticles ranged 100-150 nm were synthesised from ytterbium fibre laser ablation using the optimised range of laser power, frequency and ablation period determined from this present work. ZnO nanoparticles revealed to be porous nano-sheets structures based on TEM

[1] Present address: Fuel Cell Institute, Universiti Kebangsaan Malaysia, 43600 UKM Bangi, Selangor, Malaysia.

analysis and they are in extreme low concentration based on AAS analysis. Relatively small inhibition zones observed from antibacterial analysis due to the extreme low concentration of ZnO nanoparticles.

Keywords: Ytterbium fiber laser, Liquid-phase laser ablation, Zinc oxide nanopartices, Antibacterial activity.

1. Introduction

In recent years, nanoparticles is being explored broadly since the invention of nanotechnology as nanoparticles possess extraordinary properties, such as physic-chemical, optical and biological properties compared to their bulk material properties [1]. Their properties changed due to the decrease in size dimension to atomic level. According to Parak et al. [2], nanoparticles are one of the important finding in medical field as the biological processes occur at nanoscale and nanoparticles have the ability to amend the biological functionality of certain cells, especially bacteria strains. Bacteria strains are categorised into Gram-positive and Gram-negative bacteria, and some of them can cause human diseases. Examples of bacterial diseases are food poisoning, which is caused by *Escherichiacoli*, as well as bloodstream infections and pneumonia which caused by *Staphylococcus* aureus. Currently, metallic nanoparticles are being explored intensively as potential antibacterial agents [1]. It is known that silver and copper metals are used widely in the antibacterial applications of wound treatment and water treatment respectively since centuries ago. Other than medical field, metallic nanoparticles have potential applications in food industries, textile fabrics and water purification [1].

Zinc oxide (ZnO) nanoparticles are being investigated extensively in many recent studies due to its significant antibacterial property over a wide range of bacteria strains and it is also reported assafe and non-toxic to human by the U.S. Food and Drug administration (21CFR182.8991) [3, 4]. ZnO shows increased specific surface area due to its smaller size which further enhances the particle surface reactivity [4].Further due to its unique nature ZnO has huge potential in medical field such as drug delivery and cancer treatment, as well as in food packaging industries where they are incorporated into food packaging materials in order to inhibit the growth of food pathogens [3, 4]. It is considered as bio-safe material which possess photo oxidizing and photocatalysis impacts on both chemical and biological species [4]. Zhang et al. [5] also reported antibacterial activity of ZnO nanofluids against Escherichia coli/DH5α.

In recent years, liquid-phase laser ablation was introduced as a modified method from conventional laser ablation with the advantage of providing a rapid quenching effect on the ablated metal surfaces, concurrently to enable the ease in collection of metal nanoparticles ablated from the metal surface in the liquid medium. Liquid-phase laser ablation was first introduced in 1987, where pulsed laser was used to produce iron oxides with metastable phases from pure iron metal which was submerged in water [6]. It is a method of laser ablation in which a solid target is immersed in a liquid medium and the high power laser beam is directed through the liquid medium onto the surface of the solid target. According to the study performed by Yang [6], the species from the solid target are ejected from the surface at larger kinetic energy when the laser beam is in

contact with the target surface. The species then formed a dense regionat the solid-liquid interface, which also known as plasma. Unlike the conventional laser ablation, in liquid-phase laser ablation, the plasma in the liquid expands adiabatically at high velocity which creates extra pressure while it passes through the liquid. This high pressure in the plasma results in the increase of temperature. On the other hand, due to high temperature, some of the liquid is vaporized to form bubbles in the liquid. As more liquid is vaporized, the bubbles tend to expand until they burst at certain critical temperature and pressure. It is believed that the formation of nanocrystals or nanostructures of target is formed due to the extreme high temperature and pressure released by the collapse of the 'cavitation' bubbles [6].

Conventionally, methods for nanoparticles synthesis are solvothermal, sol-gel, water-oil microemulsion and hydrothermal. Conventional methods synthesize large quantity of nanoparticles in shorter time and require chemicals as capping agents to maintain the stability of nanoparticles [7]. However, the chemicals used are harmful to environment and tend to contaminate the nanoparticles. Liquid laser ablation is a much simpler method of synthesising nanoparticles as it does not require the usage of chemicals. Besides that, liquid laser ablation is able to produce smaller size of nanoparticles with narrower distribution and weak agglomeration; hence it is suitable for metal nanoparticles synthesis [8].

Based on the literature review, there are several areas related to liquid-phase laser ablation using fibre laser to produce nanoparticles that are yet to be explored. Most of the studies related to liquid-phase laser ablation have used Nd:YAG laser [9-15]. The use of ytterbium fibre laser in synthesising nanoparticles was found limited, however some recent studies showed that fibre laser has potential to produce comparative results with the commonly used Nd:YAG laser [8, 16]. There are various factors affecting the ZnO nanoparticles size distribution, which includes the type of liquid medium, energy fluence, wavelength, frequency, pulse duration and ablation period. Since this present study is a preliminary study of the usage of ytterbium fibre laser in synthesizing ZnO nanoparticles, only three factors: laser power, frequency and ablation period were selected due to the limitation of the specifications of fibre laser used. Studies had been done to show the effect of energy fluence of laser on the particles size and surface morphology and all are done using Nd:YAG laser [11, 13, 15]. The relationship between the energy fluence and particle size ablated is uncertain as the conclusion made by different authors, do not have the same agreement. Furthermore, there is yet any study performed on the effect of laser frequency and ablation period on the particles size distribution. ZnO nanoparticles is being investigated extensively on their antibacterial properties in more recent days as compared to silver and copper which are already known with their excellent antibacterial activity [1]. However, all studies related to the antibacterial properties of ZnO nanoparticles use either chemical or biological method to synthesis zinc oxide nanoparticles [3, 7, 17].

Hence, the objectives of this present work are to optimize the laser parameters for ZnO nanoparticles synthesis using ytterbium fibre laser and to investigate the morphology and the antibacterial activity of the ZnO nanoparticles synthesised from ytterbium fibre laser.

2. Materials and methods

2.1. Synthesis and characterisation of ZnO nanoparticles

ZnO nanoparticles were synthesised by laser ablation of zinc metal with purity of 99.99% in sterilised distilled water at room temperature. The zinc metal was placed on the metal holder which in turn was placed in the beaker. Sterilised water was poured into the beaker until the water level is 5 mm above the metal target, which was approximate 95 mL of water. ZnO nanoparticles solution was obtained by the irradiation of zinc metal with Ytterbium fibre laser (IPG Laser: YLP-1-100-20-20-HC) which operated at 1064 nm wavelength, 100 ns pulse duration and 1050 mm/s scanning speed at room temperature.

In this work, three laser parameters which are the laser power, laser frequency and ablation period were varied. As this work is a preliminary study and the selection of the range of laser parameters was uncertain, the experiment was conducted in two stages.In the first or preliminary stage of experiment, 4-level laser power (2 W, 6 W, 10 W, 14 W), 2-level laser frequency (20 kHz, 100 kHz) and 3-level ablation period (1 min, 3 min, 5 min) were applied to obtained 24 samples of ZnO nanoparticles solution. In the second or revision stage, the factors were revised by increasing the range of power to maximum (20 W), ablation period (7 min) as well as the frequency (60 kHz, 150 kHz, 200 kHz) as the results obtained in the preliminary stage were not satisfying. This stage was only carried out with the higher power region which is 14 W and 20 W. A total of 42 samples were collected from the laser ablation. The solution contained ZnO nanoparticles was turned into brown colour right after the laser ablation and turned colourless after a few hours left unstirred, as shown Fig. 1.

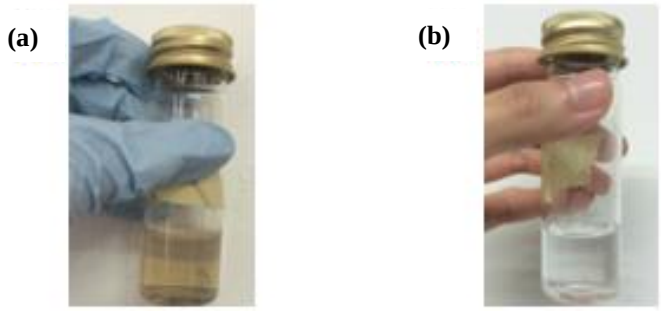

Fig. 1. Colour of the solution turned from brown (a) to colourless (b) few hours without stirring after the laser ablation.

The particle size distribution of the samples of ZnO nanoparticles solution obtained from laser ablation was investigated by Zetasizer (Malvern Nano ZS ZEN 3600). This analysis was conducted in triplicates and the average value was recorded. The sample with the best result (the smallest average size of ZnO nanoparticles) was selected for morphology analysis using TEM (Hitachi HT-7700) at 120 kV. Before undergoing TEM analysis, the sample was sonicated for 15 mins at room temperature. Then, a drop of sample is placed on a mesh copper grid support and is dried in an oven at 50 ^{o}C for 10 mins. The concentration of the

best five results of ZnO nanoparticles obtained from laser ablation was analysed by AAS (PerkinElmer AAnalyst 400) using zinc lamp.

2.2. Preparation of bacterial strains

All the procedures involving bacteria strains were conducted in the Laminar Flow Cabinet. *E. coli* strains were obtained from laboratory of School of Engineering, Taylor's University. 100 µL of *E. coli* strains were added into 100 mL of nutrient broth. The broth with bacteria strains was incubated in the Orbital Shaker Incubator (LM-400D) for overnight at 37 ºC and 100 rpm. After incubation, bacteria streaking on agar plates were done in order to obtain the isolated colony of bacteria strains. The agar plates with bacteria strains were incubated overnight at 37 ºC.

2.3. Antibacterial assay

Antibacterial activities of the best five results of ZnO nanoparticles were determined using the agar disc diffusion assay. The agar plates prepared for antibacterial assay were incubated overnight to ensure there is no contamination occurs. The isolated colony of *E. coli* was obtained from the agar plates and it was added into 100 mL of nutrient broth. The bacteria suspension was incubated in the Orbital Shaker Incubator for overnight at 37 ºC and 100 rpm. The concentration of bacteria suspension was adjusted to match the absorbance value of 0.5 McFarland turbidity standards using UV-vis spectrophotometer (Genesys 10S) with 625 nm wavelength, which the concentration of bacteria suspension is 1.5 x 10^8 colony-forming units (CFU) / mL when the absorbance value is between 0.08 to 0.1 using 625 nm wavelength. 100 µL of bacteria suspension was inoculated on the surface of nutrient agar using a sterilised glass spreaders 90º bend. Three layers of sterile filter papers with 6 mm diameter were dipped into the ZnO nanoparticles samples in order to absorb the ZnO nanoparticles onto the filter paper and they were placed on the nutrient agar with bacteria inoculated. The plates with bacteria and ZnO nanoparticles were incubated at 37 ºC for 48 hours. The inhibition zones of each sample were observed and the diameter of each inhibition zone was measured using a meter ruler. This antibacterial assay was conducted in triplicates and the average value was recorded.

3. Results and Discussion

3.1. Zinc oxide nanoparticles formation

According to previous studies [13, 14, 19, 20], ZnO nanostructures formation by liquid-phase laser ablation is divided into two types of reactions: physical and chemical reactions. When laser beam is ablated onto the zinc metal surface, a dense zinc plasma region is produced on the liquid-solid interface. The presence of liquid medium, which is distilled water in this work, creates extra pressure on the plasma and restricts the expansion of plasma hence making it denser when compared to the plasma produced by conventional laser ablation (without liquid).

The plasma expands adiabatically at high velocity until the plasma extinguished and hence zinc clusters are formed. After the disappearance of plasma, cavitation bubble is formed and expanded with time until it collapses at its maximum size. The collapse of cavitation bubble releases high temperature and pressure to the surrounding, hence it is believed that this phenomena

contributes to the formation of ZnO nanoparticles. At the same time, the zinc clusters produced from plasma react with the surrounding water medium to form zinc hydroxide, $Zn(OH)_2$ and $Zn(OH)_2$ will further decompose to form ZnO [19]. The chemical equations of the formation of $Zn(OH)_2$ and followed by formation of ZnO are shown in Eq. 1 and 2 respectively:

$$Zn + 2H_2O \rightarrow Zn(OH)_2 + H_2 \quad (1)$$

$$Zn(OH)_2 \rightarrow ZnO + H_2O \quad (2)$$

The physical and chemical reactions happened simultaneously and continuously as the laser ablation continues. The presence of ZnO nanoparticles in distilled water was justified by the colour change of the solution right after the laser ablation and few hours later, as shown in Fig. 1. The colour of solution turns brown right after the laser ablation, as shown in Fig. 1 (a) and it became colourless solution few hours later, as shown in Fig. 1 (b). This colour change is due to the extreme high temperature and pressure released from the plume produced by the large kinetic energy of the laser beam onto the metal surface [6]. The beaker containing the solution is warm when touched right after the laser ablation indicating the occurrence of the liquid-phase laser ablation mechanism. This observation is in agreement with Solati et al. [15]. At high temperature, ZnO nanoparticles formed brownish in solution and it turned into colourless after it is cooled down to room temperature.

3.2. Particle size distribution

Figure 2 shows the relationship between the average particle size of ZnO and the laser power at different frequencies with a constant ablation period of 1 min (a), 5 min (b) and 7 min (c). Figure 3 shows the relationship between the average particle size of ZnO and the laser frequency at different ablation period with a constant power of 14 W (a) and 20 W (b). Figure 4 shows the relationship between the average particle size of ZnO and the ablation period at different power with a constant frequency of 20 kHz (a), 60 kHz (b) and 100 kHz (c).

There is no general trend observed from the relationship between laser power, laser frequency and ablation time with the ZnO particle size based on the graphs shown in Fig. 2, Fig. 3 and Fig. 4. However, the factors are interconnected with each other in order to obtain the desirable particle size of ZnO nanoparticles. In Fig. 2, the samples with desirable particle size, which is below 200 nm are obtained in the higher power region, 14 W to 20 W although there is no similar trend for different frequencies and ablation periods. In Fig. 2 (a), the desirable particle sizes are observed at 10 W and 14 W at 20 kHz. At higher frequency which is 100 kHz, the particle sizes at any power are undesirable at 1 min ablation period. In Fig. 2 (b), the desirable particle sizes are observed at 14 W at both 20 kHz and 100 kHz, as well as at 20 W at 100 kHz. This shows that the increase in frequency and ablation period leads to desirable particle size at higher power region. However, the further increase of frequency does not lead to further reduction of particle size, as shown in Fig. 2 (c). Thisphenomena is clearly shown in Fig. 3, where the desirable particle sizes are obtained in the lower frequency region, 20 kHz to 100 kHz although there is no similar trend for different ablation periods and powers. In both Fig. 3 (a) and (b), the desirable particle sizes are obtained mostly from 20 kHz, 60 kHz and

100 kHz at higher power region, which is 14 W (a) and 20 W (b). It is also observed that desirable particle size is obtained at 150 kHz, 14 W but turned undesirable at the same frequency with higher power, 20W. Hence, at lower power, higher frequency can be applied in order to obtain the desirable particle size. In Fig. 4, the desirable particles sizes are obtained in the higher ablation period, 5 min to 7 min although there is no similar trend for different powers and frequencies. The desirable sizes are obtained mostly from 5 min and 7 min at lower frequency region, which is 20 kHz (a), 60 kHz (b) and 100 kHz (c). In Fig. 4 (a), the desirable particle sizes are obtained in longer ablation time (5 min and 7 min) and higher laser power (14 W and 20 W), which matches the statement concluded based on the graphs in Fig. 2. In Fig 4 (c), the desirable particle sizes are obtained from only 5 min and become undesirable at 7 min due to the higher frequency applied, 100 kHz, compared to the frequency applied in Fig. 4 (a) and (b).

Solati et al. [15] reported that the increase in laser energy fluence leads to the decrease in ZnO nanoparticles. Guillen et al. [13] reported no conclusion on the trend of ZnO nanoparticles against the laser energy fluencies. This present work showsthat the increase in laser power leads to decrease in ZnO nanoparticles, however it is strongly influenced by the other parameters: laser frequency and ablation period. Therefore, in order to obtain the desirable ZnO particle size which is less than 200 nm, the power of the ytterbium fibre laser applied should be at higher region (14 W to 20 W), lower region (60 kHz to 100 kHz) for laser frequency and higher region (5 min to 7 min) for ablation period.

Compared to previous studies done by Guillen et al. [13], Thareja et al. [14] and Solati et al. [15] which using Nd:YAG laser, the particle size of ZnO nanoparticles obtained in this study is relatively larger than the previous studies. The ZnO particle size obtained from Guillen et al. [13], Thareja et al. [14] and Solati et al. [15] are ranged 16-100 nm, 14-20 nm and 15-75 nm respectively, while the smallest particle size can be obtained from this study is 116.4 nm. Hence, in this study ZnO particles produced using Ytterbium fibre laser is larger than ZnO particles produced using Nd:YAG laser.

Fig. 2. Average ZnO particle size against laser power

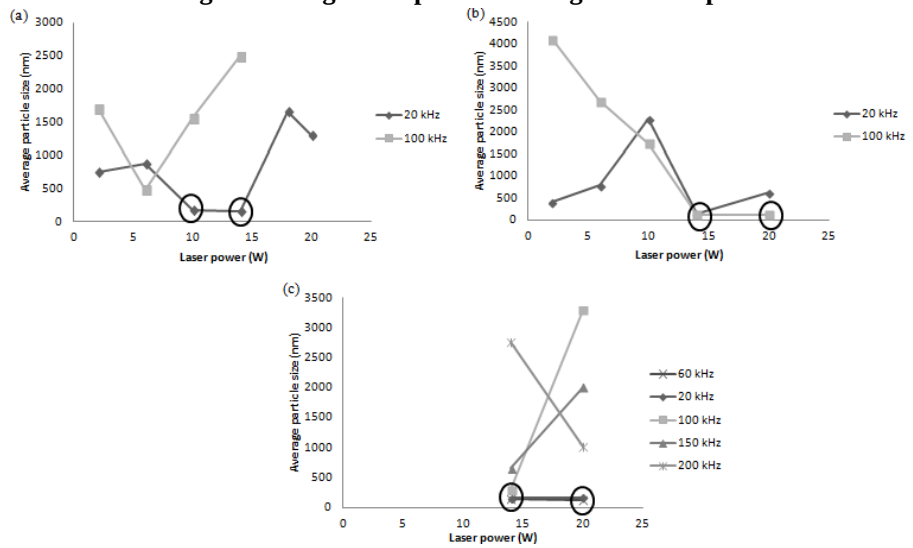

at constant 1 min (a), 5 min (b) and 7 min (c) ablation period.

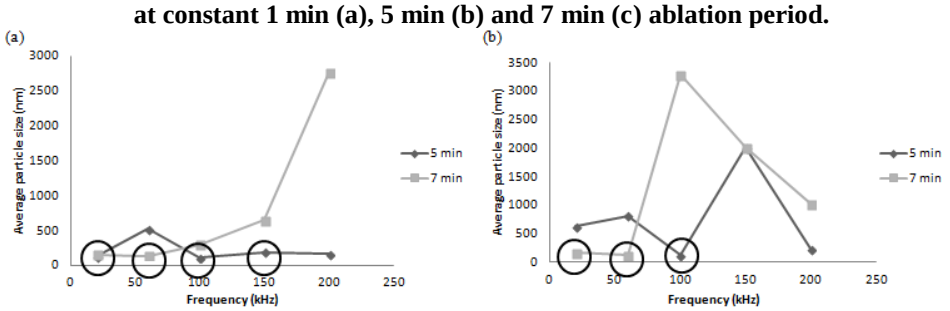

Fig. 3. Average ZnO particle size against laser frequency at constant 14 W (a) and 20 W (b) power.

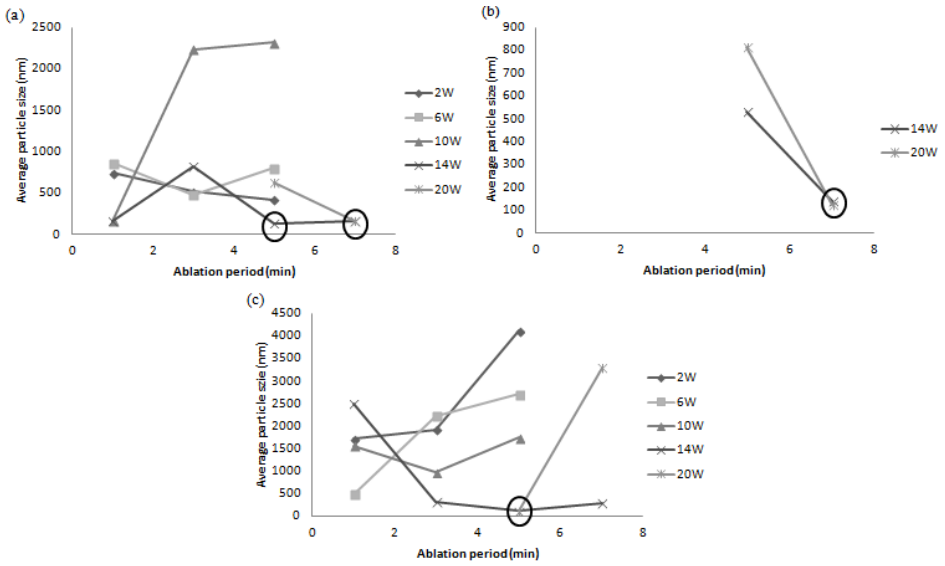

Fig. 4. Average ZnO particle size against ablation period at constant 20 kHz (a), 60 kHz (b) and 100 kHz (c) frequency.

Out of 42 samples in total, the five samples with the lowest ZnO particle size obtained from ytterbium fibre laser abltion are selected for further analysis. Table 1 shows the best five results of ZnO nanoparticles with their respective particle sizes and laser parameters. The power, frequency and ablation period ranges in Table 1 are matched with the conclusion made previously based on the graphs in Fig. 2, 3 and 4. Figure 5 shows the particle size distribution of the five samples obtained from the Zetasizer. The graphs in Fig. 5 are based on volume percentage. Although the average particle size of all the samples are above 100 nm, the greatest volume percentage of all the samples are in the range of 60-80 nm based on the graphs in Fig. 5, showing that most of the ZnO particles are in nanosize. Sample S1 and S2 even showed significant amount of nanoparticles ranged 15-40 nm. Hence, these results proved that ytterbium fibre laser can be used to synthesiseZnO particles in nanosize.

Table 1. The five lowest ZnO average particle size samples obtained from laser ablation with their respective laser parameters used.

Sample	Power (W)	Frequency (kHz)	Ablation period (min)	Average particle size (nm)
S1	14	100	5	116.4
S2	20	100	5	118.4
S3	20	60	7	123.2
S4	14	20	5	135.6
S5	14	60	7	139

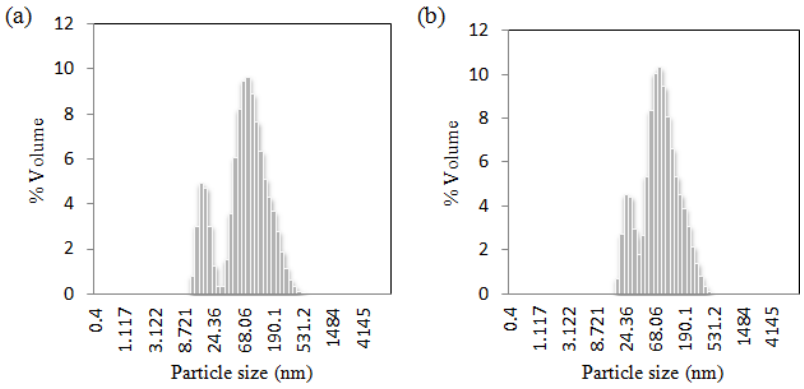

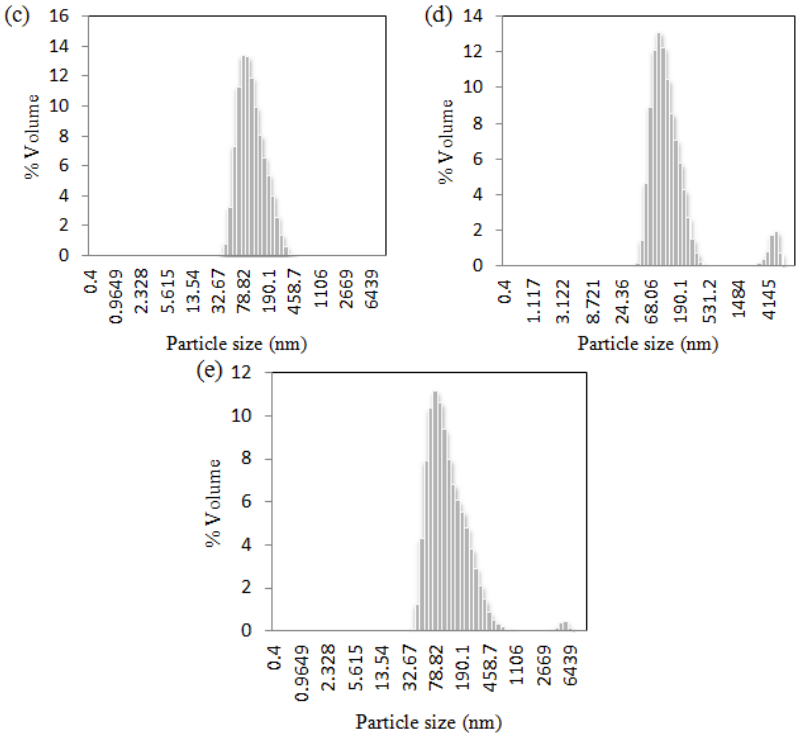

Fig. 5. Particle size distribution of the five best samples of ZnO nanoparticles obtained from ytterbium fibre laser ablation in distilled water.

3.2. Transmission electron microscopy (TEM) analysis

Figure 6 (a) and (b) show the TEM images of ZnO nanoparticles synthesised by laser ablation in distilled water. These images revealed that ZnO nanoparticles synthesised in this work are in amorphous structures. In other words, they consist of several layers nano-sheets structures attached together, which is shown by the light and dark grey region based on the TEM images. The dark grey region show denser area where more nano-sheets layers attached together, while the light grey region show less dense area where only single or a few layers of nano-sheets attached. The ZnO nanostructures obtained from ytterbium fibre laser is different from the ZnO nanostructures obtained from Nd: YAG laser in the previous studies [13-15, 21] where most of the ZnO nanoparticles produced were either spherical or flakes in shape. Furthermore, unlike the spherical ZnO which has crystalline structure, ZnO obtained from present work does not have crystalline structure with no specific shape. It is suspected that the formation of amorphous ZnO structure is due to the relatively low laser power of the ytterbium fibre laser compared to Nd: YAG laser. As lower laser power is used, a lower plasma temperature and pressure is induced during laser ablation and hence producing weaker plasma with shorter lifetime [22]. Shorter plasma lifetime leads to shorter nucleation and growth time of ZnO particles, thus forming irregular nanosheets without crystalline structure. During the formation of ZnO, the nucleation of Zn is induced by the reduction of Gibbs free energy [23]. The reduction of Gibbs free energy is necessary in order to achieve the solubility or supersaturation

equilibrium of the solute in a solution as solute above solubility equilibrium posses high Gibbs free energy. In order to lower the Gibbs free energy, solute will aggregate themselves from the solution and form a new solid phase [23]. In this case, it was observed that layers of ZnOnanosheets segregate and assemble together to reduce the free surface energy in order to reach its equilibrium state.

Figure 6 (a) shows one of the ZnO nanoparticles contained in sample S1. This quasi-spherical nano-sheet structure has approximate 77.6 nm in diameter, which is in agreement with the particle size distribution obtained from Zetasizer. Figure 6 (b) shows the close-up image of one of the ZnO nanoparticles in sample S1. Porous structures were observed from the close-up image where it is in agreement with the study done by Li et al. [18], where they showed that the ZnO which is also obtained from pulsed laser ablation using deionised water are in porous nano-sheets structures. Figure 6 (c) show the overview TEM image from one of the mesh grids, which only two particles (in red circles) were seen on a mesh grid. This shows that the concentration of ZnO nanoparticles obtained from laser ablation is very low, compared to studies done by Li et al. [18] and Solati et al. [15]. The concentration of ZnO nanoparticles obtained was further analysed using AAS which is discussed in the following section.

3.3. Atomic absorption spectroscopy (AAS) analysis

Table 2 shows the concentration of the five best results of ZnO nanoparticles obtained from ytterbium fibre laser ablation. These results reveal that the concentration of ZnO nanoparticles is ranged from 2 mg/L to 7 mg/L. Samples S3, S4 and S5 have relatively higher concentration than the samples S1 and S2. Since the power and ablation period used in these five samples are in small range, which is 14 W and 20 W for power as well as 5 min and 7 min ablation period, this may due to the lower frequency used in sample S3, S4 and S5, which is 60 kHz, 20 kHz and 60 kHz resepectively, while the frequency used in S1 and S2 are both 100 kHz. Compared to the studies by Ismail et al. [9] and Zimbone et al. [10], where the concentration of iron oxide nanoparticles by [8] and titanium oxide nanoparticles by [10] used for antibacterial analysis is 4000-4250 mg/L and 25-100 mg/L respectively, the concentration of ZnO nanoparticles obtained from ytterbium fibre laser is extremely low. It is suspected that the rate of formation of ZnO nanoparticles using ytterbium fibre laser is lower than using Nd:YAG laser due to its relatively low laser power of ytterbium fibre laser.

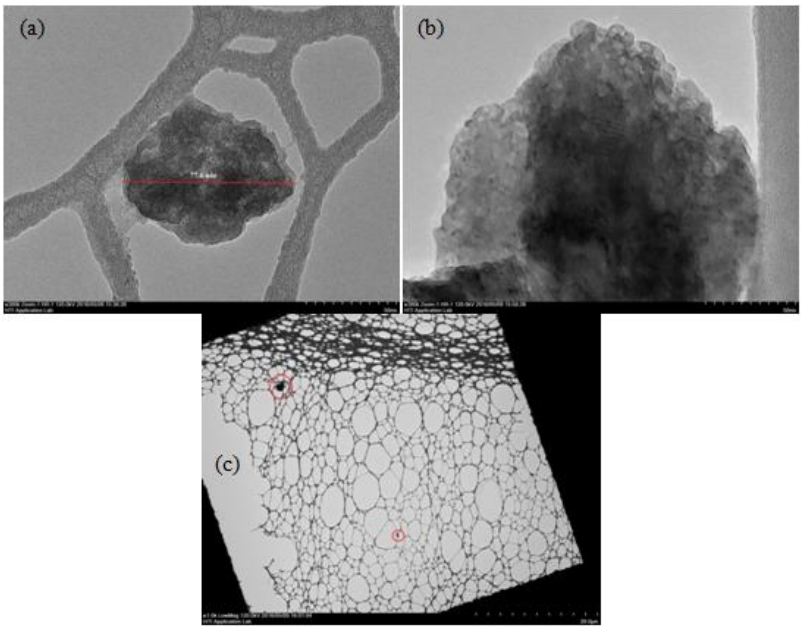

Fig. 6. TEM images of ZnO nanoparticle from sample S1 (a), close-up image of ZnO nanoparticle (b) and overview in a mesh copper grid (c).

Table 2. Concentration of the five best results of ZnO nanoparticles obtained using various laser parameters.

Sample	Concentration (mg/L)
S1	2.795
S2	2.894
S3	6.086
S4	5.665
S5	5.522

3.4. Antibacterial activity

Figure 7 shows the inhibition zones obtained from samples S1, S2 and S3 after 48 hours of incubation. The inhibition zones were indicated by relatively transparent zone surrounded the filter paper immersed with ZnO nanoparticles, as shown in black circles in Fig. 7. At nano-size scale, ZnO exhibits significant antibacterial properties compared to its bulk material properties [1]. Small particle size increases the surface area of the particles, hence they have the ability to amend the biological functionality of certain cells, especially bacteria strains [2]. It is believed that the mechanism on bacterial cell destruction of ZnO is the generation of hydrogen peroxide from ZnO surface which inhibits the bacterial growth [1, 4].

Poor antibacterial activity was seen from Fig. 7 where very small inhibition zones were observed in each sample with the diameter of 1-2 mm each. Compared to studies done by Suresh et al. [17], Anbuvannan et al. [7], the inhibition zones obtained from this work is relatively small due to the extreme low concentration of ZnO nanoparticles. The antibacterial activity of

nanoparticles is significantly affected by the nanoparticles concentration and the initial bacterial concentration [9]. Hence, the nanoparticles concentration is the major factor of their antibacterial activity in this present study. The decrease in particle size leads to increase in antibacterial activity of the nanoparticles due to the increase in large surface area of nanoparticles and hence its membrane permeability [9]. In this present study, ZnO nanoparticles in the range of 115-140 nm size are used for their antibacterial activity. Similar inhibition zones and antibacterial activities were observed which may due to the small difference between their particle sizes. Furthermore, due to their extreme low concentration, very small inhibition zones were observed in this present study.

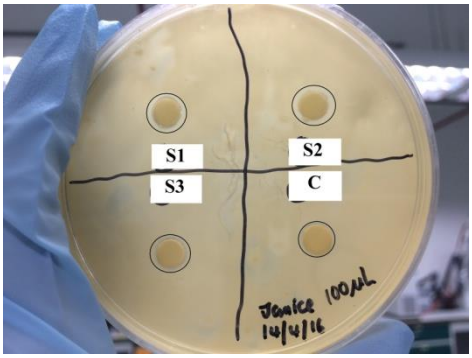

Fig. 7. Inhibition zones induced by ZnO nanoparticles in samples S1, S2 and S3 against *E. coli*.

4. Conclusion

This study revealed that zinc oxide nanoparticles were successfully produced using ytterbium fibre laser ablation in distilled water. Based on the results obtained from this present work, the most desirable ZnO average particle size, which is between 100 and 150 nm, are be synthesised using higher power region (14-20 W), lower frequency region (20-100 kHz) and longer ablation period (5-7 min). The ZnO nanoparticles are in amorphous structures, and mostly contained several layers of irregular nano-sheets structures attached together. The formation of amorphous ZnO nanostructures is suspected due to the relatively low laser power of ytterbium fibre laser compared to the commonly used Nd: YAG laser. Both TEM and AAS analysis revealed that the concentration of ZnO particles is only 2-6 mg/L, which is extremely low. The extreme low concentration of ZnO obtained from ytterbium fibre laser is also suspected due to the relatively low laser power of fibre laser used. Besides that, no significant antibacterial activity was observed from ZnO nanoparticles synthesised from ytterbium fibre laser, which may be due to the extreme low concentration of ZnO nanoparticles and the morphological dependency.

In future work to further study the feasibility of using ZnO nanoparticles produced from this method as antibacterial agent, the ablation process will be repeated in the same liquid medium using the combination of parameters obtained in this study to achieve the desired concentrations (c.a. 100 mg/L) prior to the antibacterial testing. Furthermore, to further study on other potential applications

of the ZnO nanoparticles produced from this method, the ablation process will be repeated using different liquid medium using the combination of parameters obtained from this study to study on the morphological structure of nanoparticles produced and its potential application.

References

1. Vittal, R.R. (2011). Nanoparticles and their potential application as antimicrobials. *Science against microbial pathogens: communicating current research and technological advances*, 197-209.
2. Parak, W.J.; Gerion, D.; Pellegrino, T.; Zanchet, D.; Micheel, C.; Williams, S.C.; Boudreau, R.; Le Gros, M.A.; Larabell, C.A.; and Alivisatos, A.P. (2003). Biological applications of colloidal nanocrystals. *Nanotechnology*, 14(7), 15-27.
3. Pati, R.; Mehta, R.K.; Mohanty, S.; Padhi, A.; Sengupta, M.; Vaseeharan, B.; Goswami, C.; and Sonawane, A. (2014). Topical application of zinc oxide nanoparticles reduces bacterial skin infection in mice and exhibits antibacterial activity by inducing oxidative stress response and cell membrane disintegration in macrophages. *Nanomedicine: Nanotechnology, Biology, and Medicine*, 10, 1195-1208.
4. Sirelkhatim, A. (2015). Review on zinc oxide nanoparticles: Antibacterial activity and toxicity mechanism. *Nano-Micro Letters*, 7, 219-242.
5. Zhang, L.; Ding, Y.; Povey, M.; and York, D. (2008). ZnO nanofluids - A potential antibacterial agent. *Progress in Natural Science*, 18(8), 939-944.
6. Yang, L. (2007). Chapter 2: *Liquid-phase pulsed laser ablation*. *Self-assembly and ordering nanomaterials by liquid-phase pulsed laser ablation*. University of Bristol, 33-47.
7. Anbuvannan, M.; Ramesh, M.; Viruthagiri, G.; Shanmugam, N.; and Kannadasan, N. (2015). Anisochiluscarnosus leaf extract mediated synthesis of zinc oxide nanoparticles for antibacterial and photocatalytic activities. *Materials Science in Semiconductor Processing*, 39, 621-628.
8. Boutinguiza, M.; Comesana, R.; Lusquinos, F.; Riveiro, A.; Val, J.D.; and Pou, J. (2014). Palladium nanoparticles produced by CW and pulsed laser ablation in water. *Applied Surface Science*, 302, 19-23.
9. Ismail, R.A.; Sulaiman, G.M.; Abdulrahman, S.A.; and Marzoog, T.R. (2015). Antibacterial activity of magnetic iron oxide nanoparticles synthesized by laser ablation in liquid. *Materials Science and Engineering C*, 53, 286-297.
10. Zimbone, M.; Buccheri, M.A.; Cacciato, G.; Sanz, R.; Rappazzo, G.; Boninelli, S.; Reitano, R.; Romano, L.; Privitera, V.; and Grimaldi, M.G. (2014). Photocatalytical and antibacterial activity of TiO_2 nanoparticles obtained by laser ablation in water. *Applied Catalysis B: Environmental*, 165, 487-494.
11. Mahdieh, M.H.; and Fattahi, B. (2014). Size properties of colloidal nanoparticles produced by nanosecond pulsed laser ablation and studying the effects of liquid medium and laser fluence. *Applied Surface Science*, 329, 47-57.
12. Gondal, M.A.; Qahtan, T.F.; Dastageer, M.A.; Saleh, T.A.; Maganda, Y.W.; and Anjum, D.H. (2013). Effects of oxidizing medium on the composition,

morphology and optical properties of copper oxide nanoparticles produced by laser ablation. *Applied Surface Science*, 286, 149-155.

13. Guillen, G.G.; Mendivil Palma, M.I.; Krishnan, B.; Avellaneda, D.; Castillo, G.A.; Das Roy, T.K.; and Shaji, S. (2015). Structure and morphologies of ZnO nanoparticles synthesized by pulsed laser ablation in liquid: Effects of temperature and energy fluence. *Materials Chemistry and Physics*, 162, 561-570.
14. Thareja, R.K.; and Shukla S. (2007). Synthesis and characterisation of zinc oxide nanoparticles by laser ablation of zinc in liquid. *Applied Surface Science*, 253, 8889-8895.
15. Solati, E.; Dejam, L.; and Dorranian, D. (2013). Effect of laser pulse energy and wavelength on the structure, morphology and optical properties of ZnO nanoparticles. *Optics & Laser Technology*, 58, 26-32.
16. Boutinguiza, M.; Val, J.D.; Riveiro, A.; Lusquinos, F.; Quintero, F.; Comesana, R.; and Pou, J. (2013). Synthesis of titanium oxide nanoparticles by Ytterbium fiber laser ablation. *Physics Procedia*, 41, 787-793.
17. Suresh, D.; Nethravathi, P.C.; Udayabhanu; Rajanaika, H.; Nagabhushana, H.; and Sharma, S.C. (2015). Green synthesis of multifunctional zinc oxide (ZnO) nanoparticles using Cassia fistula plant extract and their photodegradative, antioxidant and antibacterial activities. *Materials Science in Semiconductor Processing*, 31, 446-454.
18. Li, S.; Chen, M.;and Liu, X.D. (2014). Zinc oxide porous nano-cages fabricated by ablation of Zn in ammonium hydroxide. *Optics Express*, 22 (15), 18707-18714.
19. Sasaki, K. (2009). Liquid-phase laser ablation.*19th International Symposium on Plasma Chemistry*, Bochum, 1-4.
20. Chang, W.; Lin, L.; and Yu, W. (2015). Bifunctional zinc oxide nanoburger aggregates as the dye-adsorption and light-scattering layer for dye-sensitized solar cells. *Electrochimica Acta*, 169, 456-461.
21. Fazio, E.; Mezzasalma, A.M.; Mondio, G.; Neri, F.; and Saija, R. (2012). ZnO nanostructures produced by laser ablation in water: Optical and structural properties. *Applied Surface Science*, 272, 30-35.
22. Zhang, X.; Zeng, H.; and Cai, W. (2008). Laser power effect on morphology and photoluminescence of ZnO nanostructures by laser ablation in water. *Materials Letters*, 63, 191-193.
23. Cao, G. (2005). Fundamentals of homogenous nucleation. University of Washington. Retrieved June 23, 2016, from http://depts.washington.edu/solgel/documents/class_docs/MSE502/Ch_3_Section_3.2.1-3.2.5.3.pdf.